



12. PHOTOCHEMISTRY OF TM COMPLEXES

Dr. Dario Cambié

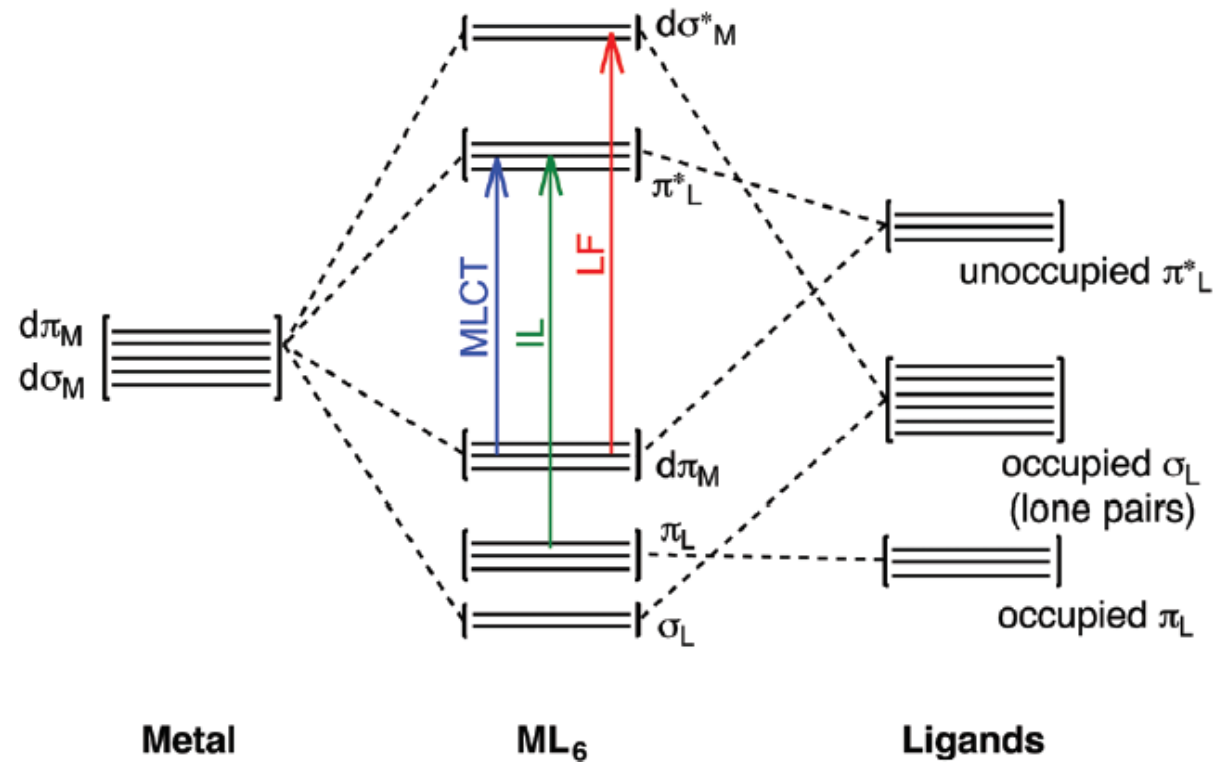
Max Planck Institute of Colloids and Interfaces

Biomolecular Systems

Dario.Cambie@mpikg.mpg.de



12.1.1 GENERAL OVERVIEW



octahedral complex w/ π -accepting ligands (like fac-Ir(ppy)₃, Ru(bpy)₃...)

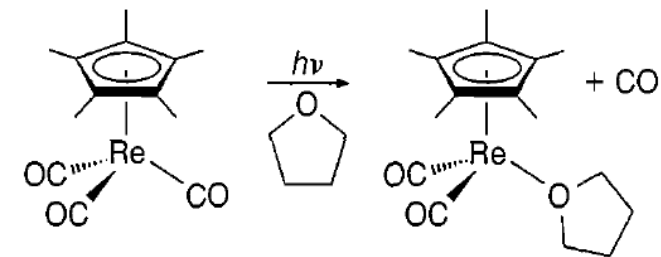
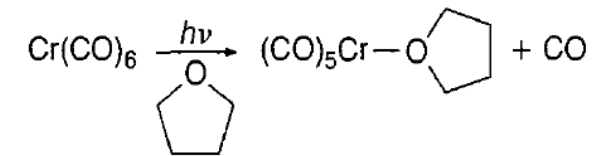
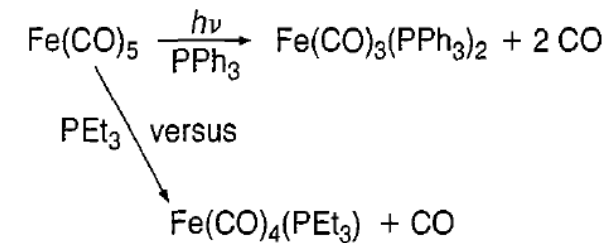
Arias-Rotondo *Chem Soc Rev* **2016** 45, 5803. DOI: [10.1039/C6CS00526H](https://doi.org/10.1039/C6CS00526H)

MacMillan *Chem Rev* **2013** 113, 5322. DOI: [10.1021/cr300503r](https://doi.org/10.1021/cr300503r)



12.2.1 LIGAND PHOTODISSOCIATION

- For better control of stoichiometry in ligand substitution (i.e. further substitution of THF after photolysis)
- Most common CO dissociation (usually w/ UV)
- Used to be considered a ligand-field d-d transition (unoccupied d to σ^*) -> weakening M-L bond...





12.2.2 LIGAND PHOTODISSOCIATION MECHANISM

Actual mechanism is more complex

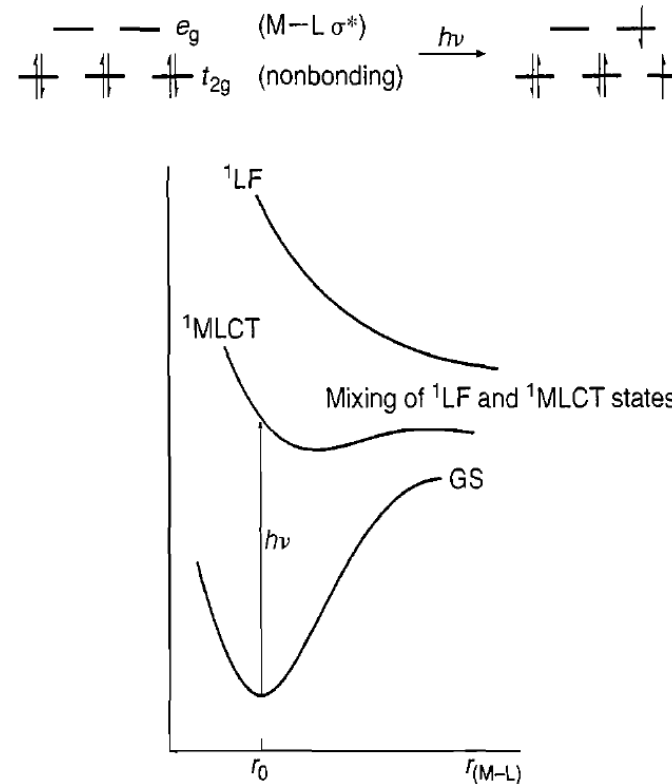


Figure 5.6.

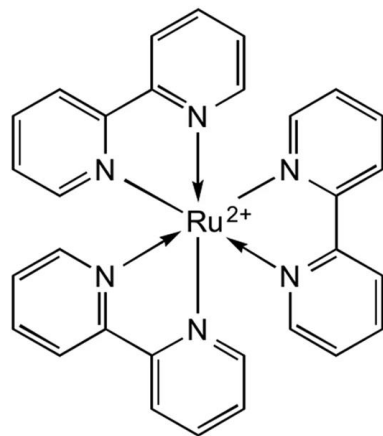
Top: Electron promotion initially thought to occur upon photolysis of an octahedral d^6 complex. Bottom: Mixing of excited states that are now thought to more accurately reflect the events that occur after photolysis of metal-carbonyl compounds, such as $M(CO)_6$ ($M = Cr, Mo, \text{ and } W$).



12.3.1 POD1

$\text{Ru}(\text{bpy})_3(\text{PF}_6)_2$ is one of the most common photoredox catalysts.

- Provide the oxidation state, d-electron count, and overall electron count for this complex.
- Propose a synthesis of this complex from inexpensive commercially available starting materials.



Photochemical Properties

Absorption λ_{max} : 454 nm

$\epsilon = 14,600 \text{ M}^{-1} \text{ cm}^{-1}$

Excited State: $^3\text{MLCT}$

Triplet Energy: 2.12 eV

τ_0 (MeCN): 1100 ns

Emission λ_{max} : 605 nm

Redox Properties

$E_{1/2}(\text{Ru}^{2+}/\text{Ru}^{3+}) = +1.29 \text{ V vs. SCE}$

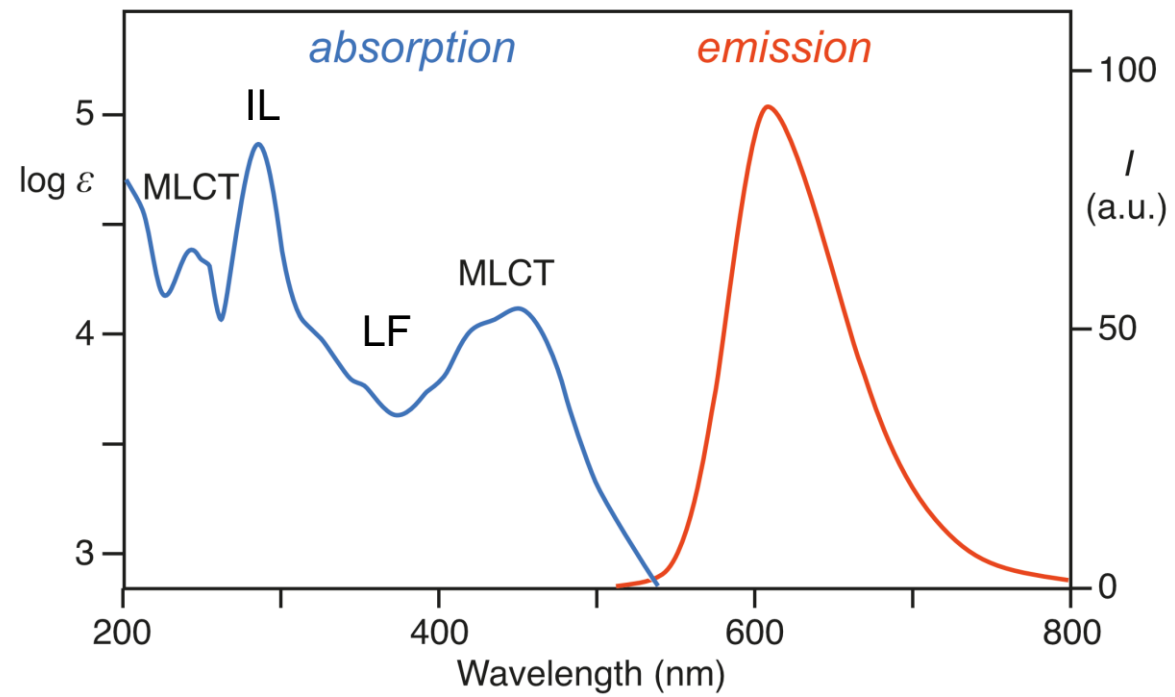
$E_{1/2}(\text{Ru}^{2+}/\text{Ru}^+) = -1.33 \text{ V vs. SCE}$

$E_{1/2}(\text{Ru}^{3+}/^*\text{Ru}^{2+}) = -0.81 \text{ V vs. SCE}$

$E_{1/2}(^*\text{Ru}^{2+}/\text{Ru}^+) = +0.77 \text{ V vs. SCE}$

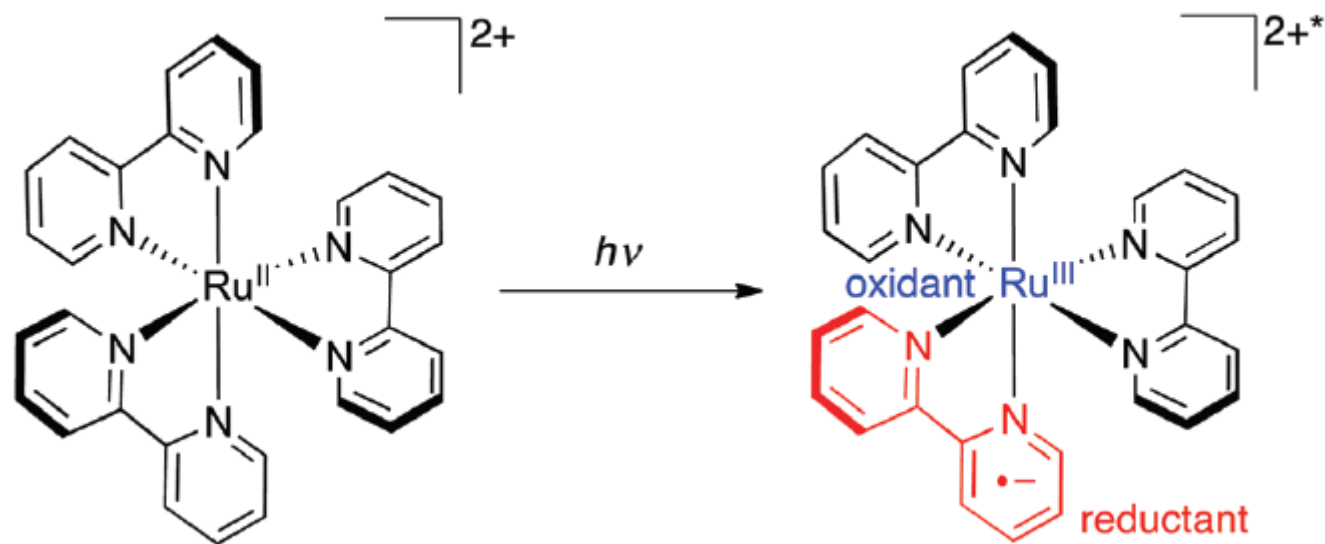


12.3.2 Ru(bpy)₃ ABSORPTION BANDS





12.3.3 Ru(bpy)₃ – EXCITED STATE



Arias-Rotondo *Chem Soc Rev* **2016** 45, 5803. DOI: [10.1039/C6CS00526H](https://doi.org/10.1039/C6CS00526H)

MacMillan *Chem Rev* **2013** 113, 5322. DOI: [10.1021/cr300503r](https://doi.org/10.1021/cr300503r)



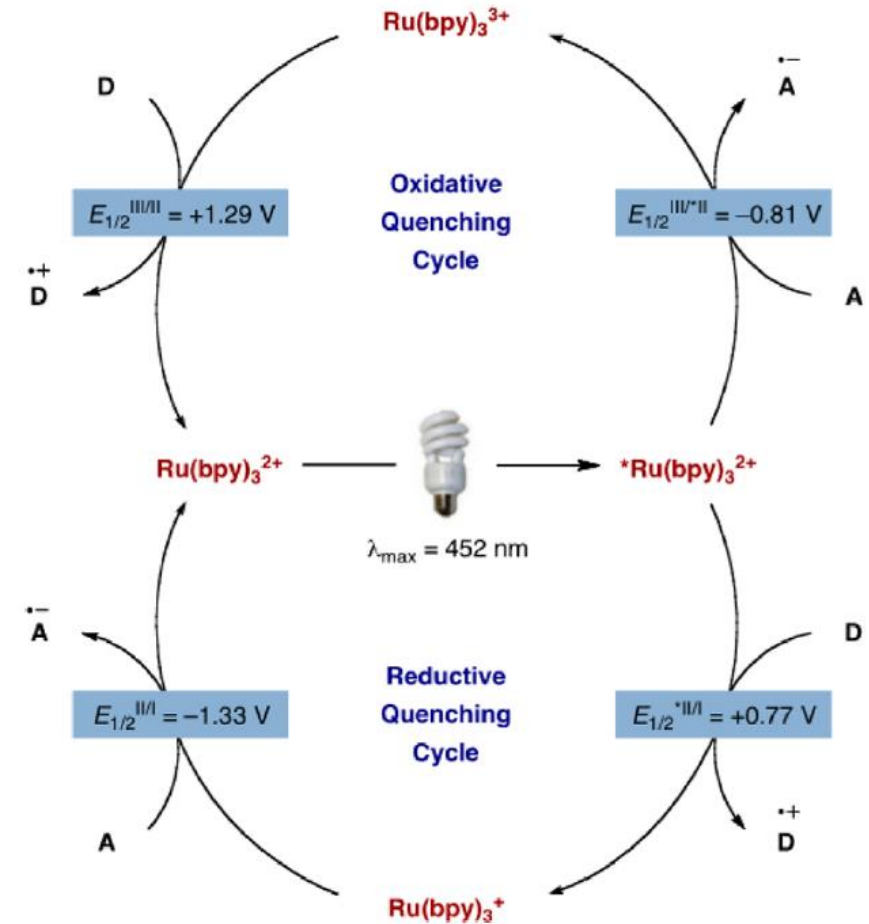
12.3.4 Ru(bpy)₃ – PHOTOCHEMISTRY

Oxidative quenchers:

viologens, polyhalomethanes, dinitro- and dicyanobenzenes, and persulfate

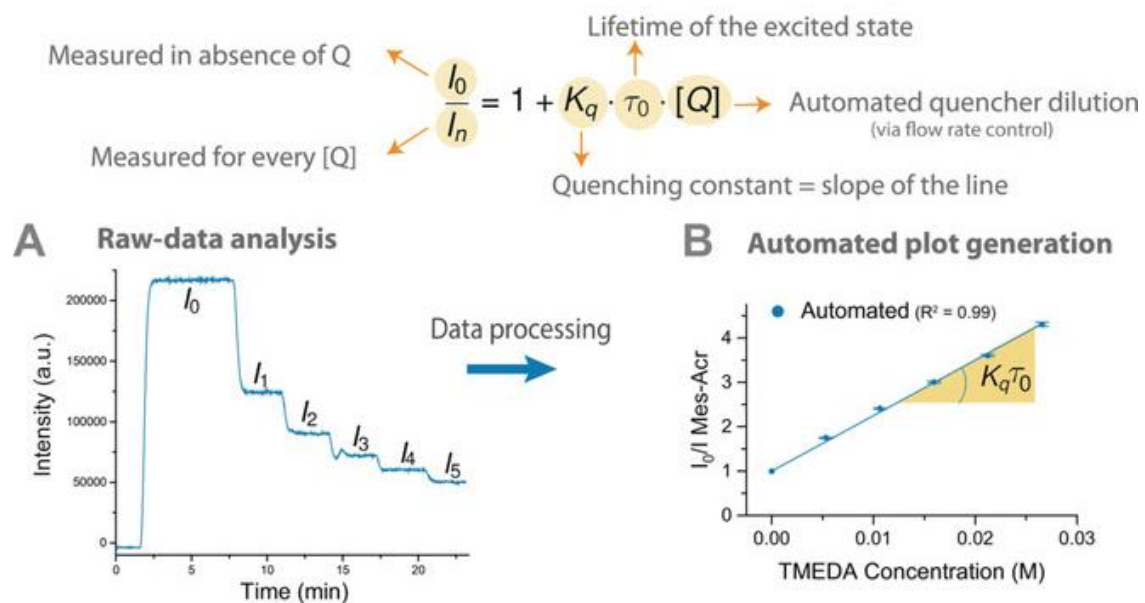
Reductive quenchers:

tertiary amines

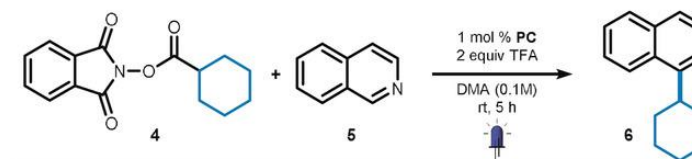




12.3.5 EXCITED STATE QUENCHING – STERN-VOLMER ANALYSIS



A Decarboxylative alkylation of N-containing heteroarenes with N-(Acyl)phthalimides

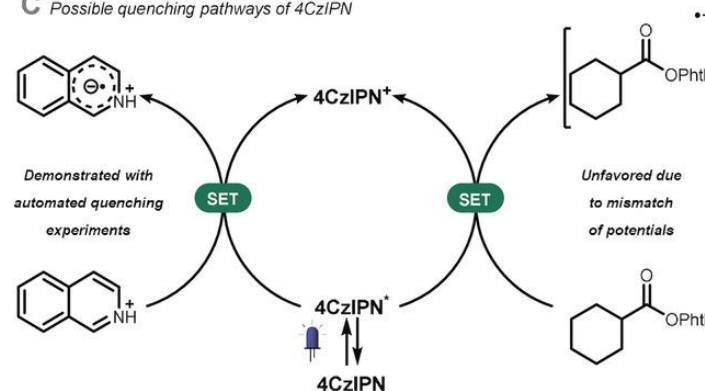


B Fluorescence quenching study

Degree of quenching: ● > 50 % ● 25 - 50 % ● < 25 %

Photocatalyst	4	5	5 + TFA	TFA
Ir(ppy) ₃	●	●	●	●
Ru(bpy) ₃ ²⁺	●	●	●	●
Mes-Acr ⁺	●	●	●	●
2CzPN	●	●	●	●
4CzIPN	●	●	●	●

C Possible quenching pathways of 4CzIPN

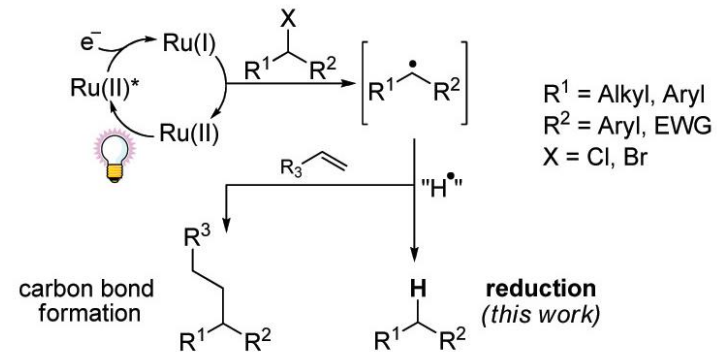
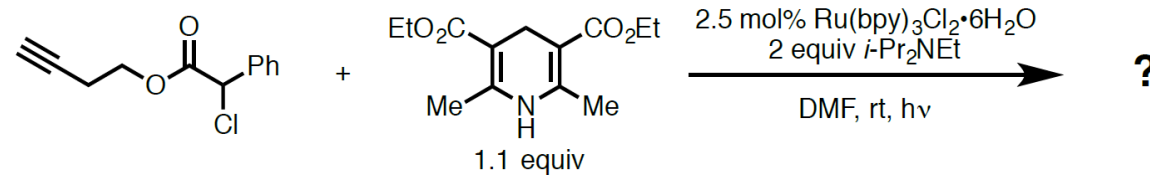


Noel *ACIE* 2018 57 11278. DOI: [10.1002/anie.201805632](https://doi.org/10.1002/anie.201805632)



POD #2

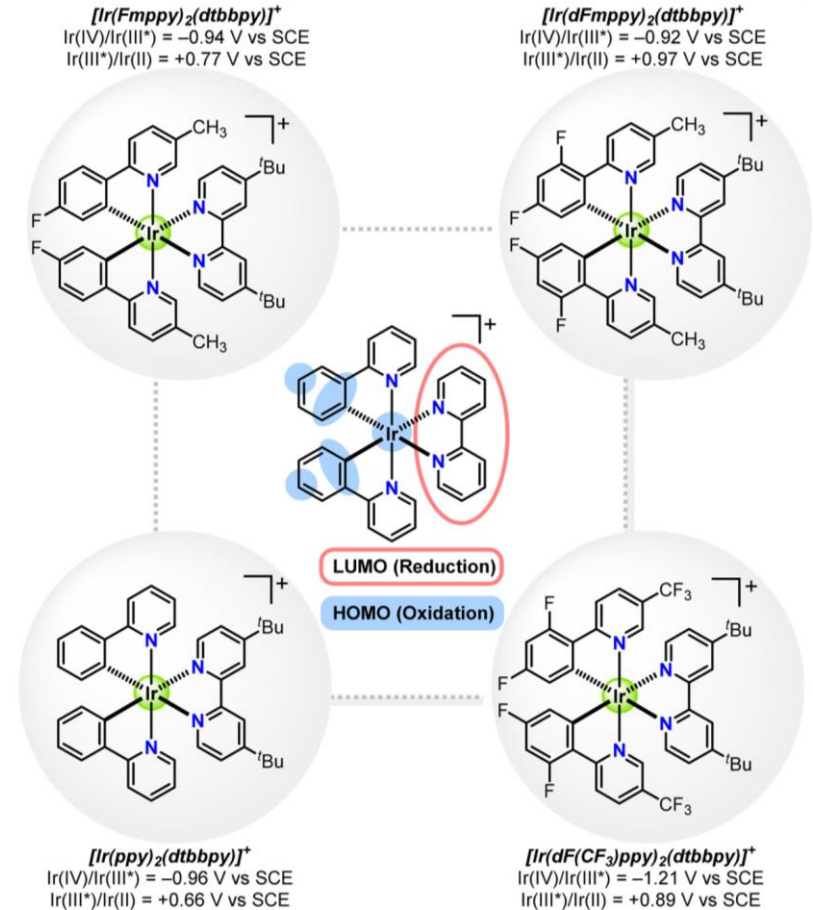
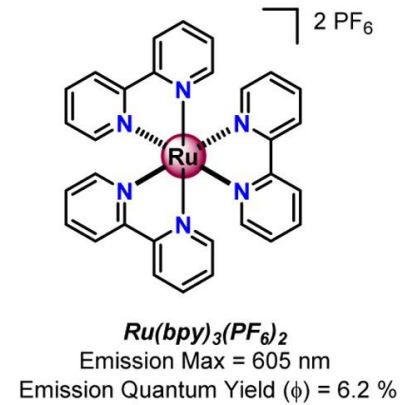
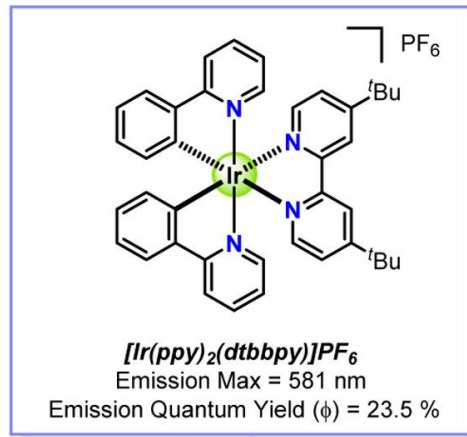
For the reaction below, **predict the product(s) and propose a plausible mechanism.**



Stephenson *JACS* **2009**, *131*, 8756. DOI: [10.1021/ja9033582](https://doi.org/10.1021/ja9033582)

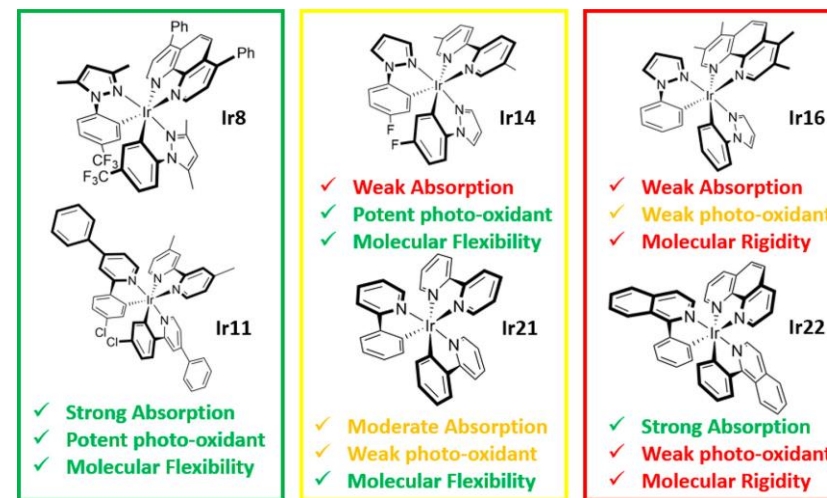
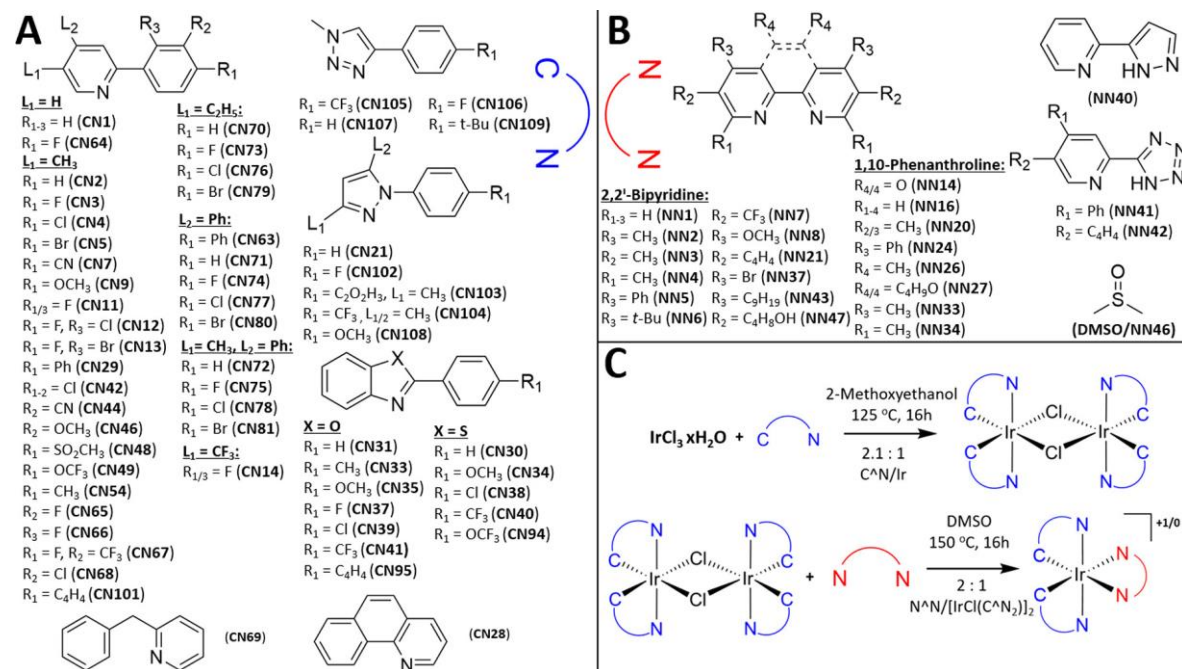


12.3.5 HETEROLEPTIC Ir PHOTOCATALYSTS





12.3.5 HETEROLEPTIC Ir PHOTOCATALYSTS

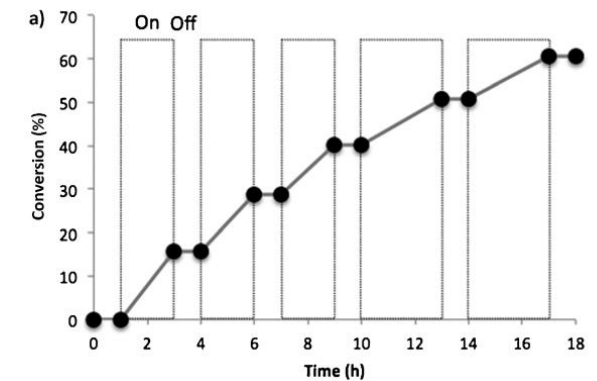
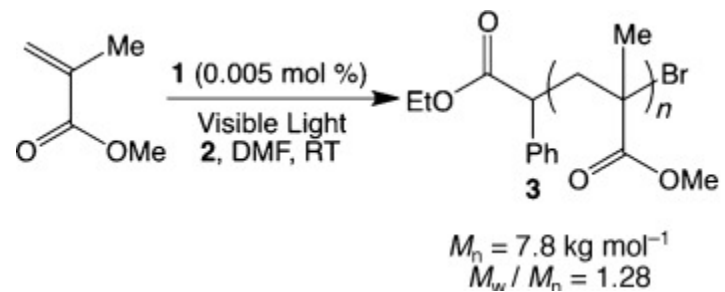


Bernhard, *JACS* **2022** 144, 1431. DOI: [10.1021/jacs.1c12059](https://doi.org/10.1021/jacs.1c12059)



12.3.5 PHOTOPOLYMERIZATION

Photochemistry for spatio-temporal control of reaction -> polymerization

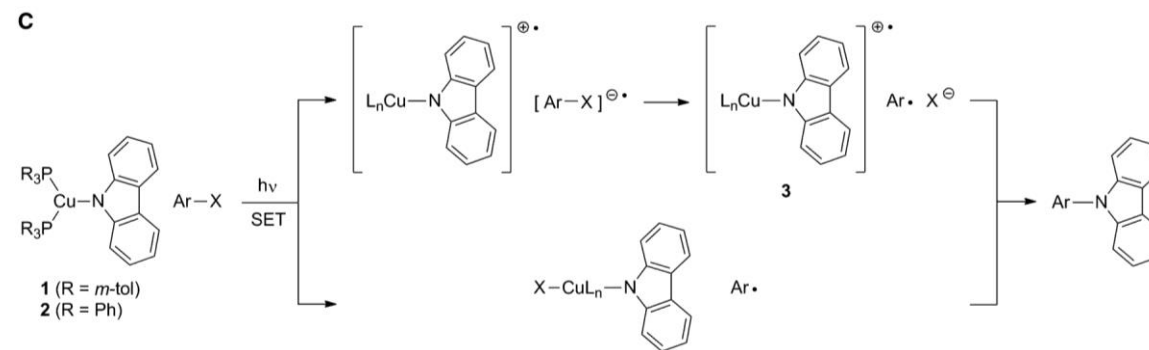
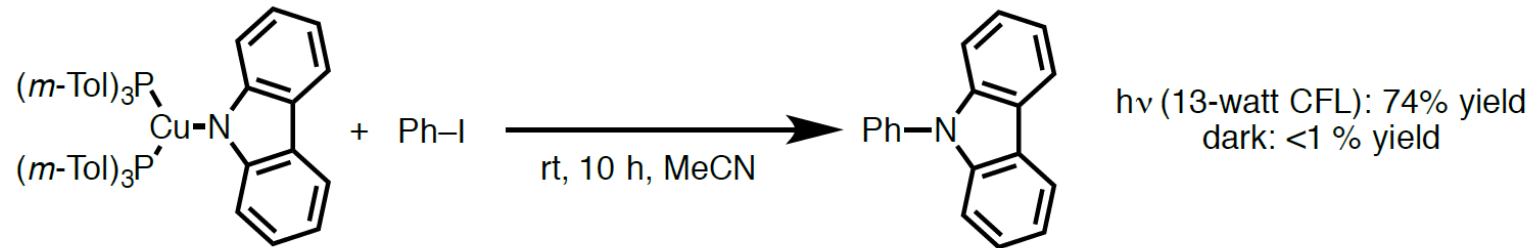


Hawker *ACIE* **2013** 51, 8850. DOI: [10.1002/anie.201203639](https://doi.org/10.1002/anie.201203639)



POD 4

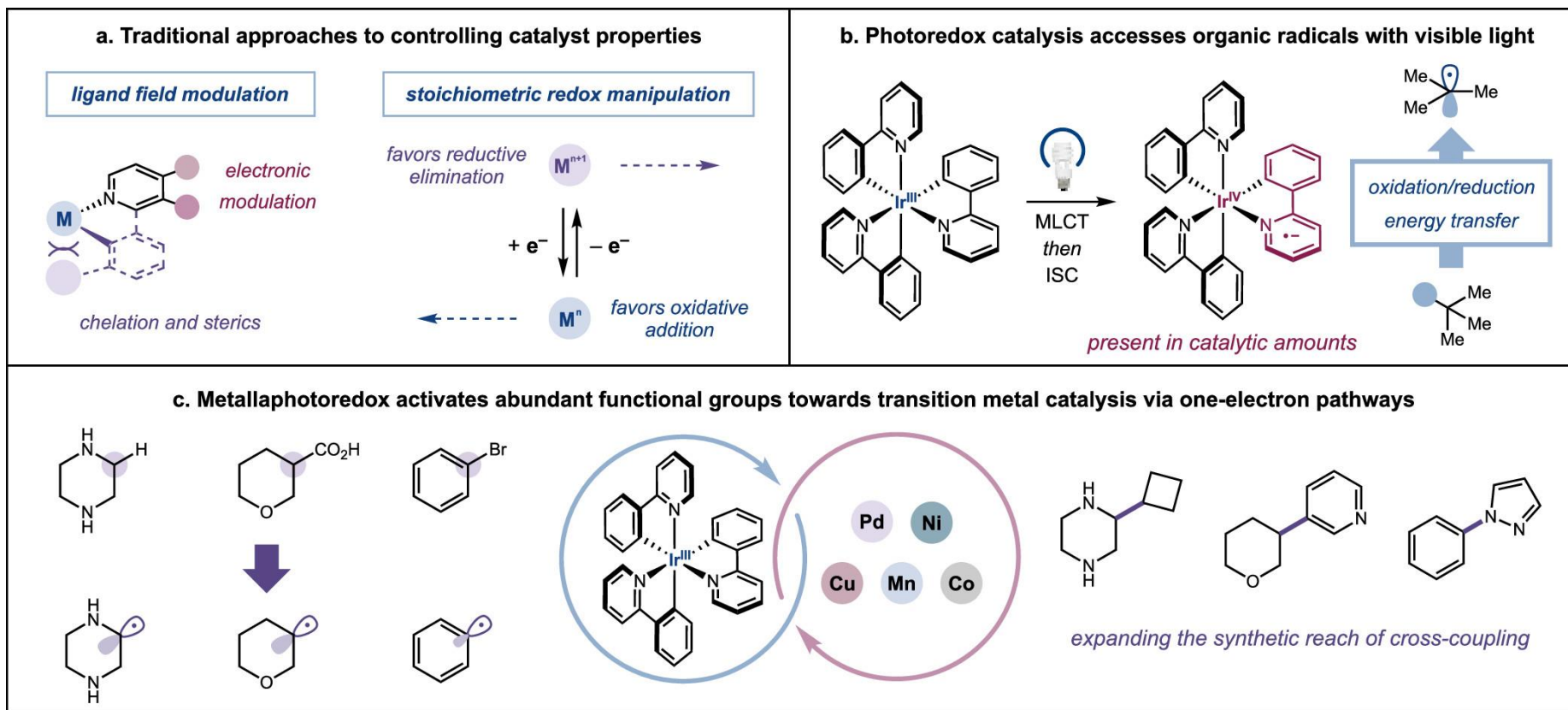
For the transformation below, **propose a role of light in the reaction.**



Fu *Science* **2012**, 338, 647. DOI: [10.1126/science.122645](https://doi.org/10.1126/science.122645)



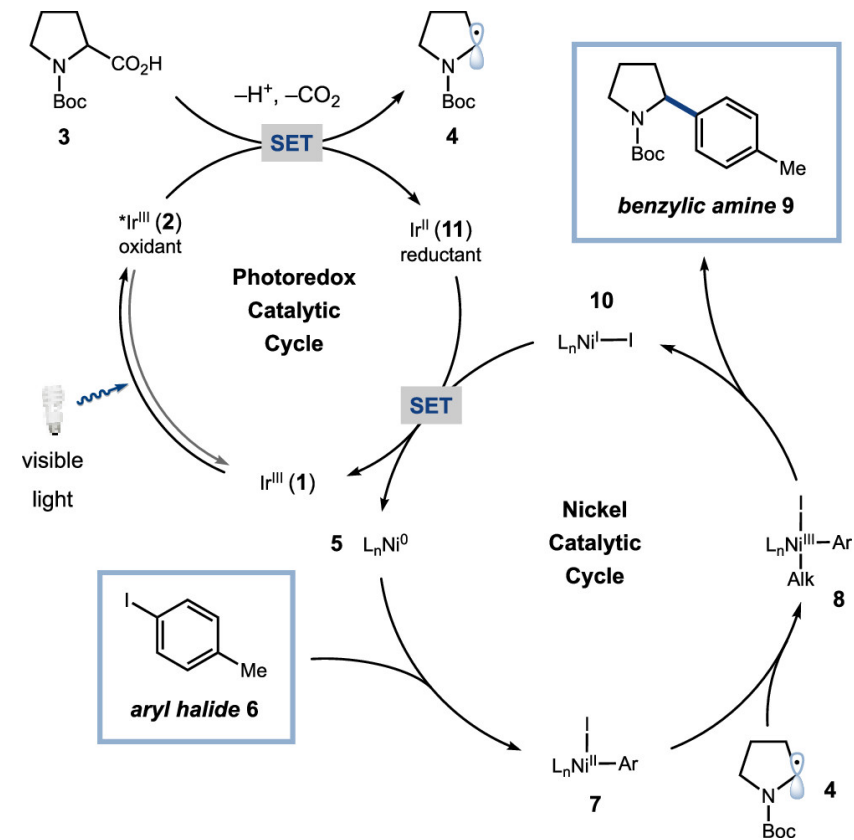
12.4.1 METALLAPHOTOREDOX



MacMillan *Chem Rev* **2022**, 122, 1485. DOI: [10.1021/acs.chemrev.1c00383](https://doi.org/10.1021/acs.chemrev.1c00383)



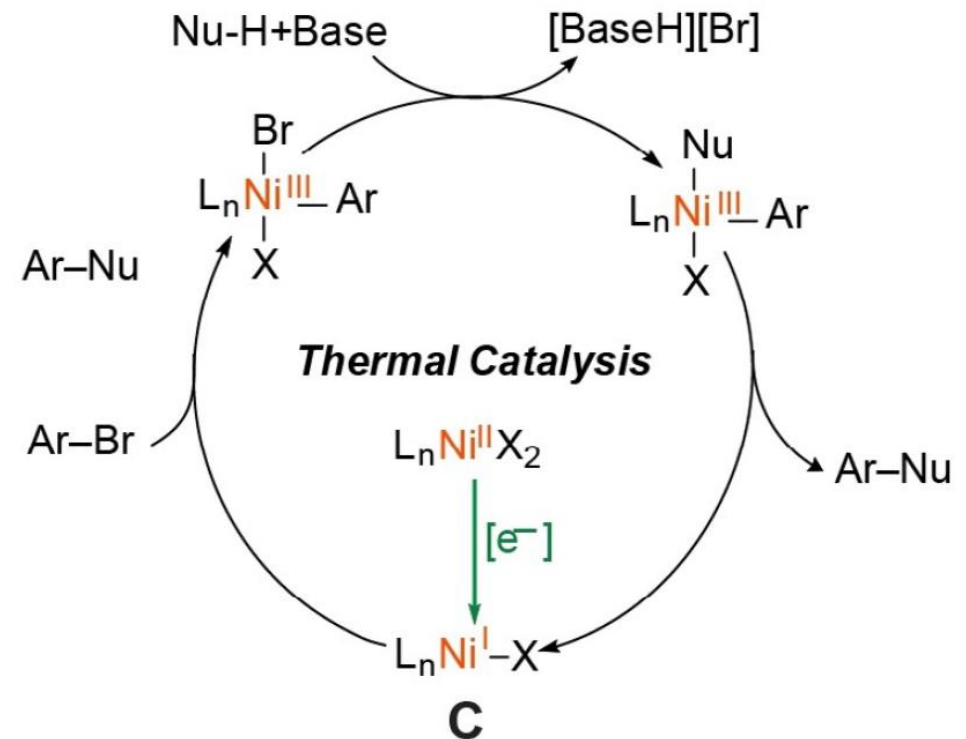
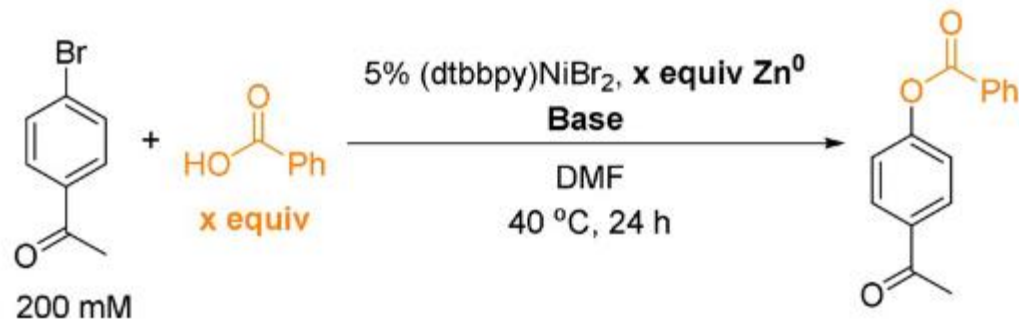
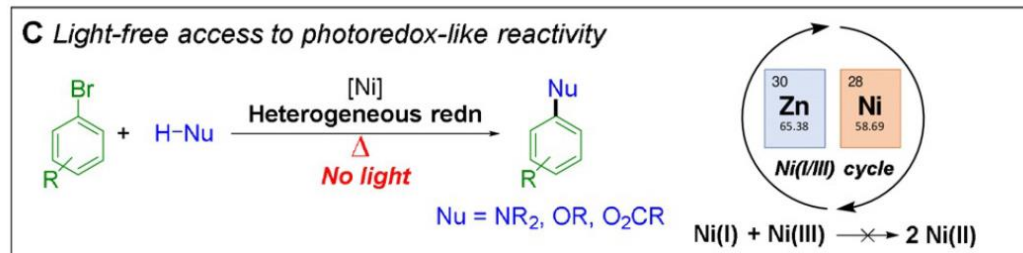
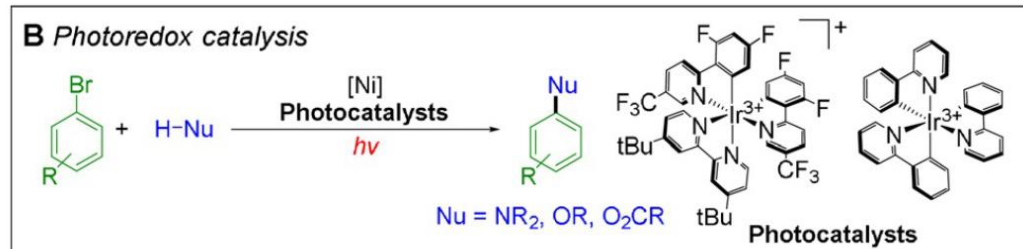
12.4.1 METALLAPHOTOREDOX



MacMillan *Chem Rev* **2022**, 122, 1485. DOI: [10.1021/acs.chemrev.1c00383](https://doi.org/10.1021/acs.chemrev.1c00383)



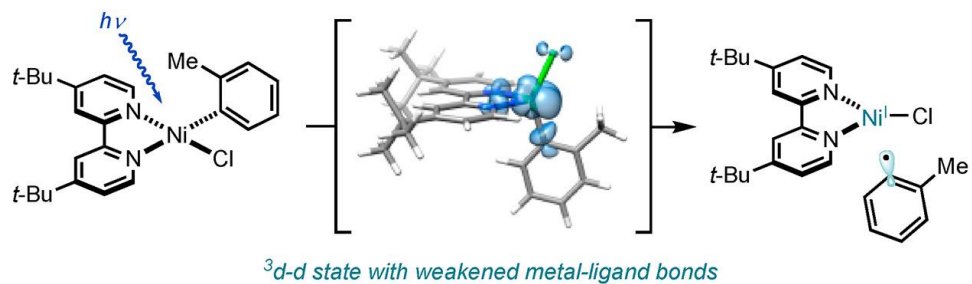
12.4.2 NICKEL: FROM PHOTO- TO THERMAL CATALYSIS



Nocera *ACIE* **2020** 59, 9527. DOI: [10.1002/anie.201916398](https://doi.org/10.1002/anie.201916398)

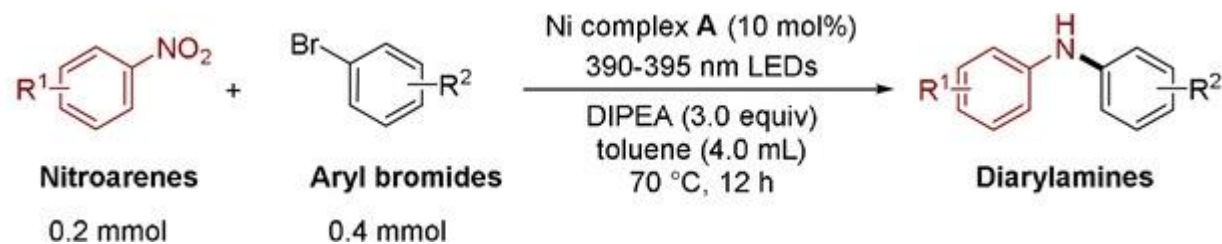


12.4.2 NICKEL: FROM PHOTO- TO THERMAL CATALYSIS

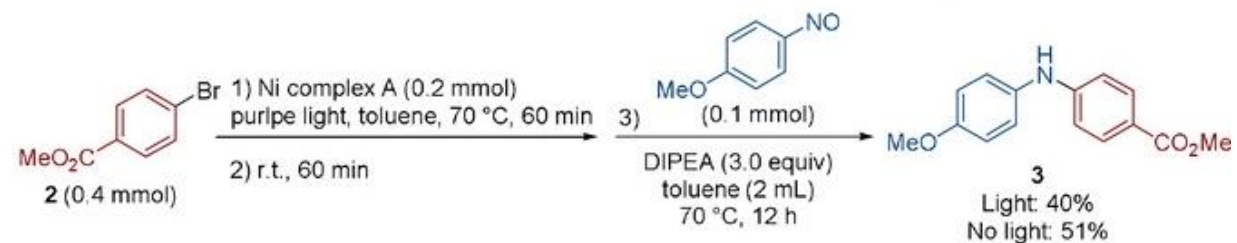


• photoinduced Ni-aryl bond homolysis

• entry into Ni(I) catalysis



(4) Direct amination of aryl bromide with nitroso compound by in-situ generated Ni(I) complex



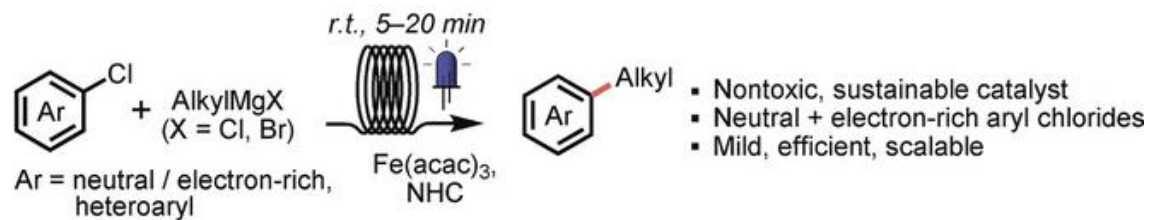
Doyle *JACS* **2020** 142, 12, 5800. DOI: [10.1021/jacs.0c00781](https://doi.org/10.1021/jacs.0c00781)

DOI: [10.1002/anie.202012877](https://doi.org/10.1002/anie.202012877)

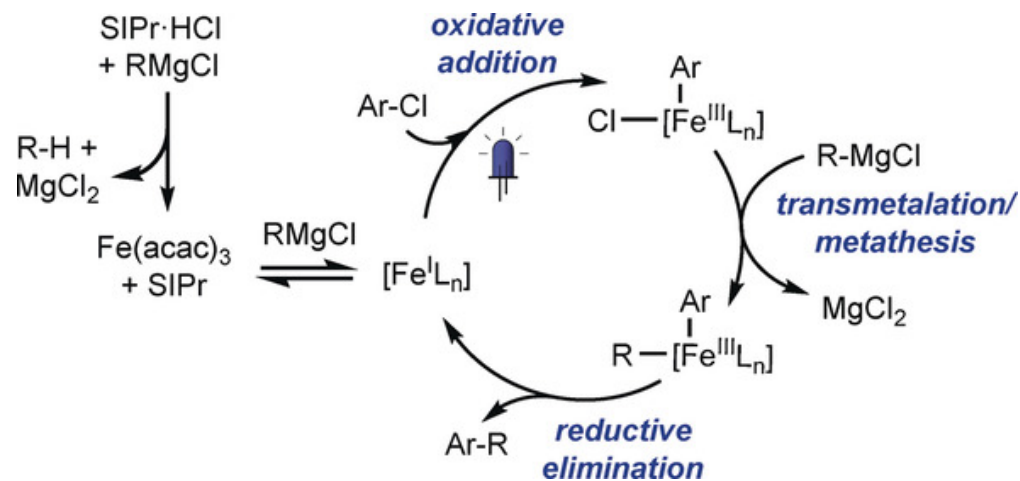
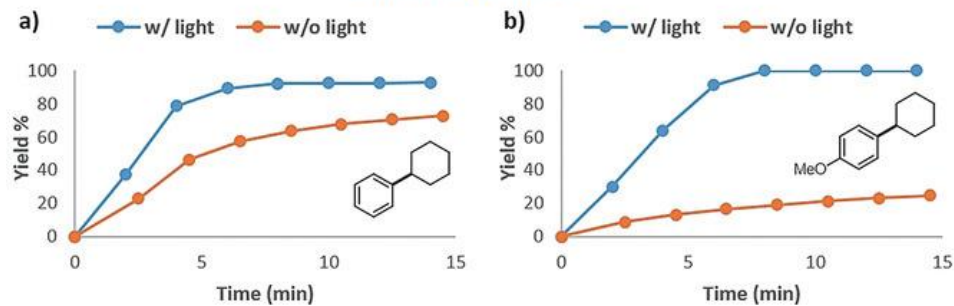


12.4.3 PHOTO-PROMOTED KUMADA

This work: Light-promoted Fe-catalyzed Kumada–Corriu cross-coupling reactions



Kinetic profiles



Noel ACIE **2019** 58 13030. DOI: [10.1002/anie.201906462](https://doi.org/10.1002/anie.201906462)